HHS Public Access

Author manuscript

Nucl Med Biol. Author manuscript; available in PMC 2015 May 01.

Published in final edited form as:

Nucl Med Biol. 2015 April ; 42(4): 381–386. doi:10.1016/j.nucmedbio.2014.12.001.

PET imaging detection of macrophages with a formylpeptide receptor antagonist

Yi Zhang, **Bijoy Kundu**, **Min Zhong**, **Tao Huang**, **Jing Li**, **Mei-Hua Chen**, **Dongfeng Pan**, **Jiang He**, and **Weibin Shi**

Department of Radiology & Medical Imaging, University of Virginia, Charlottesville, VA 22908

Abstract

Macrophages are a major inflammatory cell type involved in the development and progression of many important chronic inflammatory diseases. We previously found that apolipoprotein E-deficient ($Apoe^{-/-}$) mice with the C57BL/6 (B6) background develop type 2 diabetes mellitus (T2DM) and accelerated atherosclerosis when fed a Western diet and that there are increased macrophage infiltrations in pancreatic islets and aorta. The formyl peptide receptor 1 (FPR1) is abundantly expressed on the surface of macrophages. The purpose of this study was to evaluate the applicability of cinnamoyl-F-(D)L-F-(D)L-F (cFLFLF), a natural FPR1 antagonist, to detection of macrophages in the pancreatic islets and aorta. ^{64}Cu labeled cFLFLF and ^{18}F-fluorodeoxyglucose (FDG) were administered to mice with or without T2DM. Diabetic mice showed an increased ^{18}FDG uptake in the subcutaneous fat compared with control mice, but pancreatic uptake was minimal for either group. In contrast, diabetic mice exhibited visually noticeable more cFLFLF-^{64}Cu retention in pancreas and liver than control mice. The heart and pancreas isolated from diabetic mice contained more macrophages and showed stronger PET signals than those of control mice. Flow cytometry analysis revealed the presence of macrophages but not neutrophils in pancreatic islets. Real-time PCR analysis revealed much higher FPR1 expression in pancreatic islets of diabetic over control mice. Autoradiography and immunohistochemical analysis confirmed abundant FPR1 expression in atherosclerotic lesions. Thus, ^{64}Cu-labeled cFLFLF peptide is a more effective PET agent for detecting macrophages compared to FDG.

Keywords

PET imaging; Type 2 diabetes; Inflammation; Macrophage

Introduction

Macrophages are involved in a number of important chronic inflammatory diseases, including atherosclerosis, asthma, inflammatory bowel disease, rheumatoid, arthritis and fibrosis [1]. In these diseases, there are increased macrophage infiltrations in relevant

Correspondence: Weibin Shi, University of Virginia, Box 801339, Snyder 266, 480 Ray C Hunt Drive, Charlottesville, VA 22908, Phone: (434) 243-9420, Fax: (434) 924-9435ws4v@virginia.edu.

Disclosures

None.

tissues. In response to persistent infection or chronic insults, macrophages release inflammatory cytokines, enzymes, and growth factors, which sustain a chronic inflammatory status. Type 2 diabetes mellitus (T2DM) is a common metabolic disease whose etiology is not fully understood [2]. We and others have observed the presence of macrophages in the islets of type 2 diabetic patients and animals by histology [3][4], although the significance of locally recruited macrophages to the pathogenesis of T2DM is unclear.

^{18}F-fluorodeoxyglucose (FDG) positron emission tomography (PET) is a non-invasive imaging tool that has been used to diagnose inflammatory diseases involving macrophages. PET FDG activity has been shown an association with macrophage contents in atherosclerotic lesions [5][6][7][8]. However, due to background uptake of this tracer by other cell types, an accurate quantitation of macrophages has been difficult [9]. Thus, there is a medical need for finding more specific macrophage agents with little or no background binding to other cell types. The hexapeptide cinnamoyl-F-(D)L-F-(D)L-F (cFLFLF) is a naturally occurring antagonist to the formyl peptide receptors (FPRs), a family of G protein-coupled receptors expressed by phagocytic leukocytes [10][11]. In mammals, there are three FPR receptor subtypes, including FPR1, FPR2 and FPR3, which share significant sequence homology and are encoded by three adjacent genes. As FPRs are mainly restricted to leukocytes, the cFLFLF peptide has been used to evaluate inflammation involving neutrophils [12][13][14]. A recent study has shown that FPR1 is more abundantly expressed by macrophages than neutrophils [11]. Apolipoprotein E-deficient (Apoe$^{-/-}$) mice are a commonly used model for experimental atherosclerosis research. They develop spontaneous hyperlipidemia and atherosclerosis on a low fat chow diet. Feeding a high fat diet aggravates hyperlipidemia and promotes atherosclerosis. We have found that Apoe$^{-/-}$ mice develop T2DM when fed a Western diet [4][15][16]. Interestingly, we have observed macrophage infiltration in the islets of diabetic mice [4]. Therefore, we expected that the cFLFLF peptide could be an effective probe for monitoring macrophages in the pancreatic islets. As atherosclerotic lesions in the aorta contain macrophage-derived foam cells and few or no neutrophils [17][18], they could serve as valuable controls.

Material and Methods

Mice

Female B6.Apoe$^{-/-}$ mice were purchased from the Jackson Laboratory, Bar Harbor, ME. One group of mice were started on a Western diet containing 21% fat, 34.1% sucrose, 0.15% cholesterol, and 19.5% casein (Harlan Laboratories, TD 88137) at 6 weeks of age, and maintained on the diet for over 12 weeks. Another group was fed a chow diet throughout the entire experimental period to serve as controls. Mice were kept in a pathogen free vivarium under a 12 hour light/dark cycle, constant room temperature (22±2°C) with free access to food and water. All procedures were carried out in accordance with the National Institutes of Health guidelines and approved by the institutional Animal Care and Use Committee.

Probe labeling

The cFLFLF peptide was modified by adding a bifunctional polyethylene glycol moiety (PEG, 3.4kDa) and -2,2′,2″,2‴-(1,4,7,10-tetraazacyclododecane-1,4,7,10-tetrayl) tetraacetic

acid (DOTA) motif through a lysine (K) spacer, as reported [12]. The resulting compound was capable of binding Cu^{2+}. 4–6 mCi (148–222 MBq) of $^{64}CuCl_2$ was incubated with 20 mg of cFLFLF-PEG-DOTA in 0.1N ammonium acetate (pH 5.5) buffer at 40°C for 20 min. The mixture was then purified on semipreparative RP HPLC to collect fractions containing cFLFLFK-PEG-DOTA-^{64}Cu.

PET Imaging

Mice were anesthetized by intramuscular injection of ketamine (80 mg/kg) and xylazine (8 mg/kg) before they were injected via the tail veins with 7–10 MBq of ^{18}FDG or 18–25 MBq of radiolabelled peptide (5–10 μg) in 200 μl of saline per mouse. Anesthesia lasted approximately 1 h. Anesthetized mice were kept on a warm pad before and after scan. PET scans were performed using Siemens Focus 120 microPET 2 h after ^{18}F-FDG injection or 24 h after injection of the peptide. Immediately following PET scans, the heart and pancreas of mice were removed, and PET scans were then conducted on the isolated organs. PET images were constructed for regions of interest using the OSEM-MAP algorithm [19].

Histology and Immunohistochemistry

The heart and adjacent aorta were fixed in 10% formalin and processed with the standard histological procedure. Atherosclerotic lesions in the aortic root were determined by oil red stain, as we previously reported [20][21]. The presence of macrophages in the aortic root was detected with a rat antimouse macrophage/monocyte IgG (Serotec) as previously reported [22]. FPR1 expression was detected with a goat antibody from Santa Cruz Biotechnology, Inc.

^{64}Cu-cFLFLF autoradiography

^{64}Cu-cFLFLF binding to atherosclerotic lesions was evaluated by autoradiography. Cryosections of the aortic root with atherosclerotic lesions were incubated with ^{64}Cu-cFLFLF for 1 h, then washed thoroughly with PBS before being exposed to X-ray films. Adjacent cryosections were stained with oil red O, and alignment of autoradiographic and oil red O images allowed estimation of ^{64}Cu radioactivity in atherosclerotic plaques and the adjacent aortic wall without plaques. **Pancreatic islet cell preparation, flow cytometric analysis, and real-time PCR**. Pancreatic islets were prepared as we reported [4]. Briefly, the pancreas was perfused in situ, first with saline through the heart and then with a solution containing collagenase XI via the common bile duct. The entire pancreas was then isolated and digested in the collagenase XI-containing solution. Digested pancreas was filtered to capture islets. For flow cytometry, theislets prepared were further digested into individual cells with a mixture of collagenases XI and I. Islet cells were stained with fluorophore-conjugated primary antibodies, including BV421-conjugated rat anti-mouse LY-6G (BD Biosciences), Alexa 488-conjugated rat anti-mouse CD11b (BD Biosciences), APC-conjugated anti-mouse CD45 (eBioscience), and PE-conjugated anti-mouse Mac3 (eBioscience). Stained cells were analyzed on a FACSCalibur flow cytometry using FlowJo software. The macrophage content was defined as cells double positive for CD11b and Mac3 on a CD45-positive gate. Neutrophils were identified as cells positive for LY-6G and CD11b on a CD45-positive gate. The mRNA expression level of FPR1 relative to GAPDH

mRNA in the islets of mice was determined by real-time PCR. Total RNA was extracted from the islets, treated with DNase I, and reverse transcribed to cDNA using ThermoScript RT-PCR system (Invitrogen). cDNA was used as template for amplification of FPR1 and GAPDH using a SYBR Green supermix reagent on a CFX Real-Time PCR Detection System (Bio-Rad). The primers for FPR1 amplification were 5′-GCACCAATTTGGGGACCAAC-3′/5′-GCTGGAAGTTAGAGCCCGTT-3′, and were 5′-GAGGCCGGTGCTGAGTATGT-3′/5′-AAGGGTGGAGCCAAAAGGGTCATC-3′ for GAPDH.

Statistical analysis

Values were expressed as means ± SD, with *n* indicating the number of mice. Student's t test was used for determining statistical significance between diabetic and non-diabetic mice. Differences were considered statistically significant at $P < 0.05$.

RESULTS

Development of type 2 diabetes

We previously reported that Apoe$^{-/-}$ mice with the B6 background develop T2DM on the Western diet [4]. In this study, blood glucose levels of B6.Apoe$^{-/-}$ mice were measured with a glucometer using whole blood squeezed from the cut tail tip. On a chow diet, B6.Apoe$^{-/-}$ mice had a fasting blood glucose level of 76 ± 12 mg/dl (n = 15; Figure 1). After being fed a Western diet for 12 weeks, their fasting glucose levels rose to 115±17 mg/dl (n = 7). The elevation in blood glucose was highly significant (P=0.00045).

PET imaging

PET scans were performed 2 h after tail vein injection of ^{18}F-FDG. The most distinct difference between control and diabetic mice was the signal from the subcutaneous adipose tissue: the diabetic mice showed a high ^{18}F-FDG uptake while the uptake was barely detectable in the control mice (Figure 2). The standardized uptake value (SUV) of the diabetic mice (n=4) was 0.529±0.157, significantly higher than the value of 0.182±0.013 in the control mice (n=3) (P=0.0139). ^{18}F-FDG uptake was not detectable in the liver or heart of control mice, but it was observable in these organs of diabetic mice. Both control and diabetic mice showed abundant ^{18}F-FDG accumulation in the kidneys. No signal was observed in regions of the pancreas for either control or diabetic mice.

For the cFLFLF peptide, PET scans were performed 24 h after its administration. Similar to^{18}F-FDG, cFLFLFK-PEG-^{64}Cu showed the highest accumulation in the kidneys of both control and diabetic mice (Figure 3). Accumulation of the tracer in the pancreas differed dramatically between control and diabetic mice: no signal was detectable in the pancreas of control mice while a strong signal was observed in the pancreas of diabetic mice. In addition, the tracer showed more retention in the liver of diabetic mice than of control mice.

To confirm the in vivo finding, the pancreas and heart were removed from the mice and PET scans were performed on these isolated organs. Consistent with the in vivo finding, the pancreas isolated from the diabetic mice showed stronger signal than the pancreas of control

mice (Figure 4). The heart isolated from diabetic mice also showed more tracer retention than the heart of control mice. Atherosclerotic lesions in the aortic root, which contained numerous macrophages, were evaluated by classic oil red O staining and immunostaining targeting macrophages and FPR1 (Figure 5). As diabetic mice were fed the Western diet, they developed much larger atherosclerotic lesions than control mice fed a chow diet. Immunostaining showed the abundance of macrophages in the lesions. FPR1 was primarily expressed in atherosclerotic lesions, specically in those newly formed lesions with high-density macrophage infiltration. FPR1 expression was barely observed in the necrotic area of atherosclerotic lesions. The autoradiography of an aortic root section showed a good agreement between the radioactivity of ^{64}Cu-cFLFLFK and the presence of atherosclerotic lesions (Figure 6). Flow cytometry was carried out to assess the presence of macrophages and neutrophils in the pancreatic islets of B6.apoE$^{-/-}$mice fed the Western diet. Macrophages were identified as CD11b and Mac3 double positive cells and neutrophils were identified as CD11b and LY-6G double positive cells following positive selection for the common leukocyte antigen CD45. Macrophages accounted for 2.9% of all living islet cells, but no neutrophils were detectable (0%) (Figure 7A). Real-time PCR was performed to determine the difference between control and diabetic mice in FPR1 mRNA expression levels in the islets. The ratio of FPR1 to GAPDH in mRNA expression levels was 0.866 in diabetic mice, but it was 0.066 in control mice (Figure 7B).

Discussion

The cFLFLF peptide has been shown to be an effective PET imaging agent for detecting neutrophils in vivo [13]. It binds to the FPR receptors on the surface of the cells with a high binding affinity and acts as an antagonist [13]. As the FPR receptor is more abundantly expressed by macrophages, in this study we used a type 2 diabetic mouse model to test the potential of the cFLFLF peptide as a PET agent to detect macrophages in vivo. We have now demonstrated the effectiveness for this peptide as a PET agent to image macrophages.

Apoe$^{-/-}$ mice are a commonly used animal model for atherosclerosis research. They develop spontaneous hyperlipidemia and all phases of atherosclerotic lesions in large and medium-size arteries even when fed a low-fat chow diet [18]. Feeding of a high-fat diet aggravates hyperlipidemia and promotes plaque growth [18][23][24]. As atherosclerotic lesions contain numerous macrophages but have no neutrophils, the heart with atherosclerosis is obviously a perfect control for testing the effectiveness of a ligand for imaging macrophages. A much stronger PET signal with the peptide was observed for the heart isolated from diabetic mice, which had larger atherosclerotic lesions, as compared to the heart of non-diabetic mice, which had smaller lesions. Similarly, the pancreas of diabetic mice had more macrophages and exhibited a stronger PET signal with the peptide than the pancreas of non-diabetic mice that had fewer macrophages [4]. Using flow cytometry, we have demonstrated the presence of macrophages but not neutrophils in the pancreatic islets of Apoe$^{-/-}$ mice fed the Western diet. Through immunohistochemical analysis, we have demonstrated the co-localization of macrophages and FPR1 in atherosclerotic lesions. Thus, the enhanced PET signals from the heart and the pancreas of diabetic mice with the cFLFLF peptide should be attributable to the increased numbers of macrophages in these organs, although there was a possibility for the up-regulation of the FPR receptor in the heart and pancreas by the high-fat diet feeding.

A relatively high ^{64}Cu-cFLFLF accumulation was observed in the liver of diabetic mice. This finding could be explained by increases numbers of macrophages in the liver due to inflammatory responses induced by the high-fat diet. The liver has a large number of macrophage lineage cells, Kupffer cells, which make up 80% of the total body macrophages under physiological conditions [25][26]. A recent study has shown that the population of Kupffer cells increases in mice fed a high-fat diet [27]. Nevertheless, there was a possibility that an up-regulated expression of the FPR receptor in the liver by the high-fat diet. A high retention of the tracer was observed in the kidneys of both diabetic and non-diabetic mice. This was probably due to the renal clearance of ^{64}Cu-cFLFLF.

The subcutaneous fat exhibited a higher FDG uptake in the mice that were fed the Western diet than those fed the chow diet. This finding is in agreement with our previous observation that Apoe$^{-/-}$ mice on the Western diet have no impairment in insulin sensitivity [4]. As such, higher blood glucose levels are expected to lead to more glucose absorbed by peripheral tissues. The finding on an increased FDG uptake by the liver of mice on the Western diet supports this speculation. The adipose tissue contains a number of macrophages [28][29], which could also contribute to increased glucose uptake by subcutaneous fat of mice fed the Western diet.

Despite the presence of macrophages in the pancreas, this study has failed to visualize FDG uptake by this organ in those mice fed the Western diet. A probable explanation is that even though the pancreas of diabetic mice contained a number of macrophages, which were expected to augment FDG uptake, their contribution to overall FDG uptake was small and could be overwhelmed by the greater mass of other cellular components within this organ. ^{18}F-FDG is considered the gold standard tracer that has been used for clinical applications to diagnose a number of diseases, including atherosclerosis [30]. This study has shown that the cFLFLF peptide is superior to FDG in imaging macrophages and could be used to visualize the pathological processes involving macrophages.

Acknowledgments

Sources of Funding: This study was supported by NIH grant DK097120.

References

1. Wynn TA, Chawla A, Pollard JW. Macrophage biology in development, homeostasis and disease. Nature. 2013; 496:445–455. [PubMed: 23619691]
2. Wolford JK, Vozarova de Courten B. Genetic basis of type 2 diabetes mellitus: implications for therapy. Treat Endocrinol. 2004; 3:257–267. [PubMed: 16026108]
3. Ehses JA, Perren A, Eppler E, Ribaux P, Pospisilik JA, Maor-Cahn R, Gueripel X, Ellingsgaard H, Schneider MK, Biollaz G, Fontana A, Reinecke M, Homo-Delarche F, Donath MY. Increased number of islet-associated macrophages in type 2 diabetes. Diabetes. 2007; 56:2356–2370. [PubMed: 17579207]
4. Li J, Wang Q, Chai W, Chen MH, Liu Z, Shi W. Hyperglycemia in apolipoprotein E-deficient mouse strains with different atherosclerosis susceptibility. Cardiovasc Diabetol. 2011; 10:117. [PubMed: 22204493]
5. Tawakol A, Migrino RQ, Bashian GG, Bedri S, Vermylen D, Cury RC, Yates D, LaMuraglia GM, Furie K, Houser S, Gewirtz H, Muller JE, Brady TJ, Fischman AJ. In vivo 18F-fluorodeoxyglucose

positron emission tomography imaging provides a noninvasive measure of carotid plaque inflammation in patients. J Am Coll Cardiol. 2006; 48:1818–1824. [PubMed: 17084256]

6. Rudd JH, Myers KS, Bansilal S, Machac J, Rafique A, Farkouh M, Fuster V, Fayad ZA. (18)Fluorodeoxyglucose positron emission tomography imaging of atherosclerotic plaque inflammation is highly reproducible: implications for atherosclerosis therapy trials. J Am Coll Cardiol. 2007; 50:892–896. [PubMed: 17719477]
7. Rudd JH, Myers KS, Bansilal S, Machac J, Woodward M, Fuster V, Farkouh ME, Fayad ZA. Relationships among regional arterial inflammation, calcification, risk factors, and biomarkers: a prospective fluorodeoxyglucose positron-emission tomography/computed tomography imaging study. Circ Cardiovasc Imaging. 2009; 2:107–115. [PubMed: 19808576]
8. Zhang Z, Machac J, Helft G, Worthley SG, Tang C, Zaman AG, Rodriguez OJ, Buchsbaum MS, Fuster V, Badimon JJ. Non-invasive imaging of atherosclerotic plaque macrophage in a rabbit model with F-18 FDG PET: a histopathological correlation. BMC Nucl Med. 2006; 6:3. [PubMed: 16725052]
9. Folco EJ, Sheikine Y, Rocha VZ, Christen T, Shvartz E, Sukhova GK, Di Carli MF, Libby P. Hypoxia but not inflammation augments glucose uptake in human macrophages: Implications for imaging atherosclerosis with 18fluorine-labeled 2-deoxy-D-glucose positron emission tomography. J Am Coll Cardiol. 2011; 58:603–614. [PubMed: 21798423]
10. Rabiet MJ, Huet E, Boulay F. The N-formyl peptide receptors and the anaphylatoxin C5a receptors: an overview. Biochimie. 2007; 89:1089–1106. [PubMed: 17428601]
11. Gemperle C, Schmid M, Herova M, Marti-Jaun J, Wuest SJ, Loretz C, Hersberger M. Regulation of the formyl peptide receptor 1 (FPR1) gene in primary human macrophages. PLoS One. 2012; 7:e50195. [PubMed: 23185575]
12. Zhang Y, Kundu B, Fairchild KD, Locke L, Berr SS, Linden J, Pan D. Synthesis of novel neutrophil-specific imaging agents for Positron Emission Tomography (PET) imaging. Bioorg Med Chem Lett. 2007; 17:6876–6878. [PubMed: 17959381]
13. Locke LW, Chordia MD, Zhang Y, Kundu B, Kennedy D, Landseadel J, Xiao L, Fairchild KD, Berr SS, Linden J, Pan D. A novel neutrophil-specific PET imaging agent: cFLFLFK-PEG-64Cu. J Nucl Med. 2009; 50:790–797. [PubMed: 19372473]
14. Xiao L, Zhang Y, Liu Z, Yang M, Pu L, Pan D. Synthesis of the Cyanine 7 labeled neutrophil-specific agents for noninvasive near infrared fluorescence imaging. Bioorg Med Chem Lett. 2010; 20:3515–3517. [PubMed: 20488705]
15. Su Z, Li Y, James JC, Matsumoto AH, Helm GA, Lusis AJ, Shi W. Genetic linkage of hyperglycemia, body weight and serum amyloid-P in an intercross between C57BL/6 and C3H apolipoprotein E-deficient mice. Hum Mol Genet. 2006; 15:1650–1658. [PubMed: 16595606]
16. Li J, Lu Z, Wang Q, Su Z, Bao Y, Shi W. Characterization of Bglu3, a mouse fasting glucose locus, and identification of Apcs as an underlying candidate gene. Physiol Genomics. 2012; 44:345–351. [PubMed: 22274563]
17. Koltsova EK, Hedrick CC, Ley K. Myeloid cells in atherosclerosis: a delicate balance of anti-inflammatory and proinflammatory mechanisms. Curr Opin Lipidol. 2013; 24:371–380. [PubMed: 24005215]
18. Nakashima Y, Plump AS, Raines EW, Breslow JL, Ross R. ApoE-deficient mice develop lesions of all phases of atherosclerosis throughout the arterial tree. Arterioscler Thromb. 1994; 14:133–140. [PubMed: 8274468]
19. Locke LW, Berr SS, Kundu BK. Image-derived input function from cardiac gated maximum a posteriori reconstructed PET images in mice. Mol Imaging Biol. 2011; 13:342–347. [PubMed: 20521133]
20. Su Z, Li Y, James JC, McDuffie M, Matsumoto AH, Helm GA, Weber JL, Lusis AJ, Shi W. Quantitative trait locus analysis of atherosclerosis in an intercross between C57BL/6 and C3H mice carrying the mutant apolipoprotein E gene. Genetics. 2006; 172:1799–1807. [PubMed: 16387874]
21. Li Y, Gilbert TR, Matsumoto AH, Shi W. Effect of aging on fatty streak formation in a diet-induced mouse model of atherosclerosis. J Vasc Res. 2008; 45:205–210. [PubMed: 18063868]

22. Yuan Z, Pei H, Roberts DJ, Zhang Z, Rowlan JS, Matsumoto AH, Shi W. Quantitative trait locus analysis of neointimal formation in an intercross between C57BL/6 and C3H/HeJ apolipoprotein E-deficient mice. Circ Cardiovasc Genet. 2009; 2:220–228. [PubMed: 19718279]

23. Shi W, Wang NJ, Shih DM, Sun VZ, Wang X, Lusis AJ. Determinants of atherosclerosis susceptibility in the C3H and C57BL/6 mouse model: evidence for involvement of endothelial cells but not blood cells or cholesterol metabolism. Circ Res. 2000; 86:1078–1084. [PubMed: 10827138]

24. Tian J, Pei H, James JC, Li Y, Matsumoto AH, Helm GA, Shi W. Circulating adhesion molecules in apoE-deficient mouse strains with different atherosclerosis susceptibility. Biochem Biophys Res Commun. 2005; 329:1102–1107. [PubMed: 15752767]

25. Seki S, Habu Y, Kawamura T, Takeda K, Dobashi H, Ohkawa T, Hiraide H. The liver as a crucial organ in the first line of host defense: the roles of Kupffer cells, natural killer (NK) cells and NK1.1 Ag+ T cells in T helper 1 immune responses. Immunol Rev. 2000; 174:35–46. [PubMed: 10807505]

26. Doherty DG, O'Farrelly C. Innate and adaptive lymphoid cells in the human liver. Immunol Rev. 2000; 174:5–20. [PubMed: 10807503]

27. Shono S, Habu Y, Nakashima M, Sato A, Nakashima H, Miyazaki H, Kinoshita M, Tsumatori G, Shinomiya N, Seki S. The immunologic outcome of enhanced function of mouse liver lymphocytes and Kupffer cells by high-fat and high-cholesterol diet. Shock. 2011; 36:484–493. [PubMed: 21937954]

28. Weisberg SP, McCann D, Desai M, Rosenbaum M, Leibel RL, Ferrante AW Jr. Obesity is associated with macrophage accumulation in adipose tissue. J Clin Invest. 2003; 112:1796–1808. [PubMed: 14679176]

29. Pereira SS, Teixeira LG, Aguilar EC, Matoso RO, Soares FL, Ferreira AV, Alvarez-Leite JI. Differences in adipose tissue inflammation and oxidative status in C57BL/6 and ApoE−/− mice fed high fat diet. Anim Sci J. 2012; 83:549–555. [PubMed: 22776793]

30. Glaudemans AW, Quintero AM, Signore A. PET/MRI in infectious and inflammatory diseases: will it be a useful improvement? Eur J Nucl Med Mol Imaging. 2012; 39:745–749. [PubMed: 22297458]

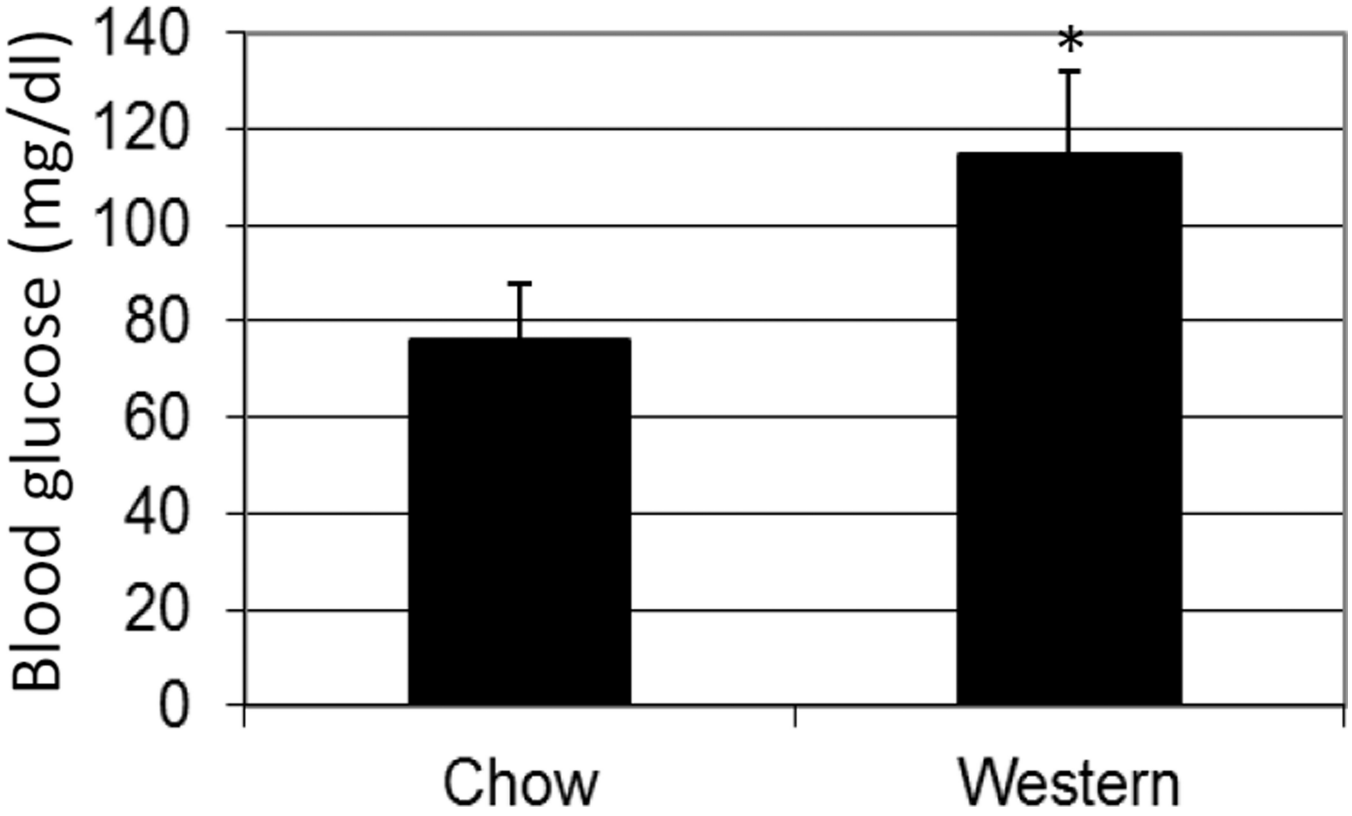

Figure 1.

Fasting blood glucose levels of female B6.Apoe$^{-/-}$mice fed a chow or Western diet. Mice were fasted overnight before blood glucose concentrations were determined with a glucometer using whole blood taken from the cut tail tips. Values are means ± SD of 7 or 15 mice. * $P < 0.05$ vs. mice fed a chow diet.

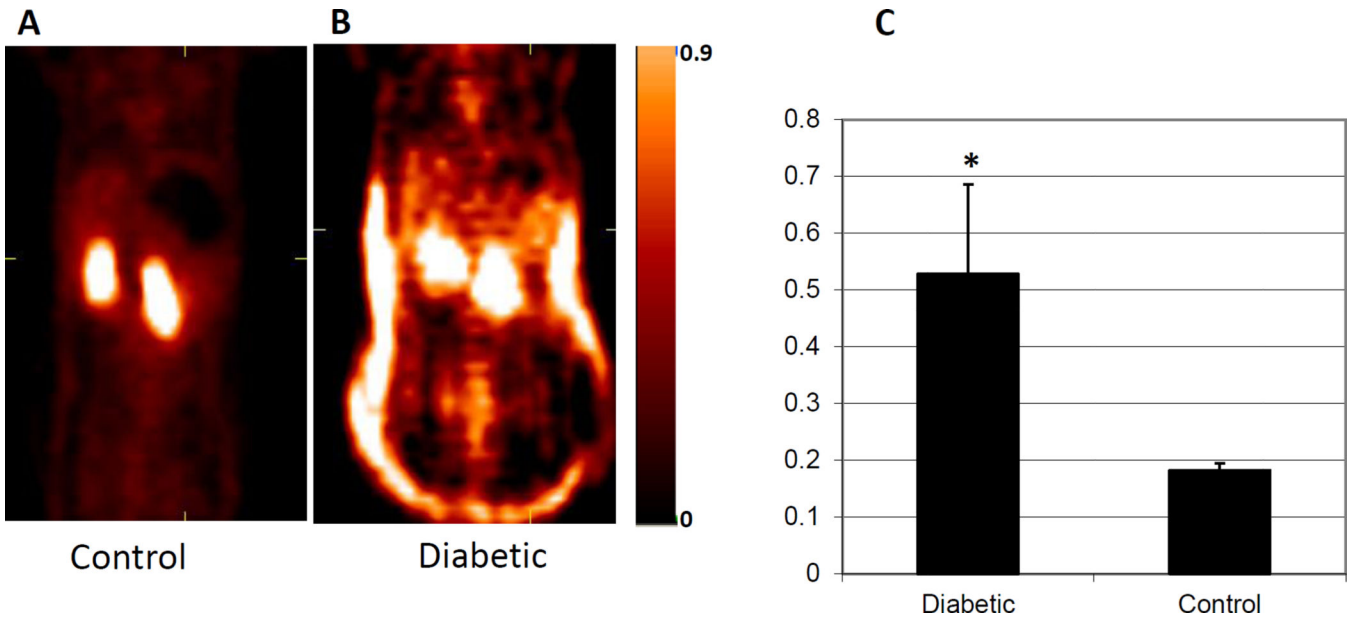

Figure 2.

PET images obtained 2 h after administration of ^{18}F-FDG to control and diabetic mice. 7–10 MBq ^{18}F-FDG was injected via the tail veins. Diabetic mice showed an increased ^{18}F-FDG uptake by the subcutaneous fat and the liver, compared to control mice. A, control mouse; B, diabetic mouse; C, the standardized uptake value (SUV) of FDG in the subcutaneous fat of control and diabetic mice. Results are means ± SD of 3 or 4 mice per group. * P<0.05.

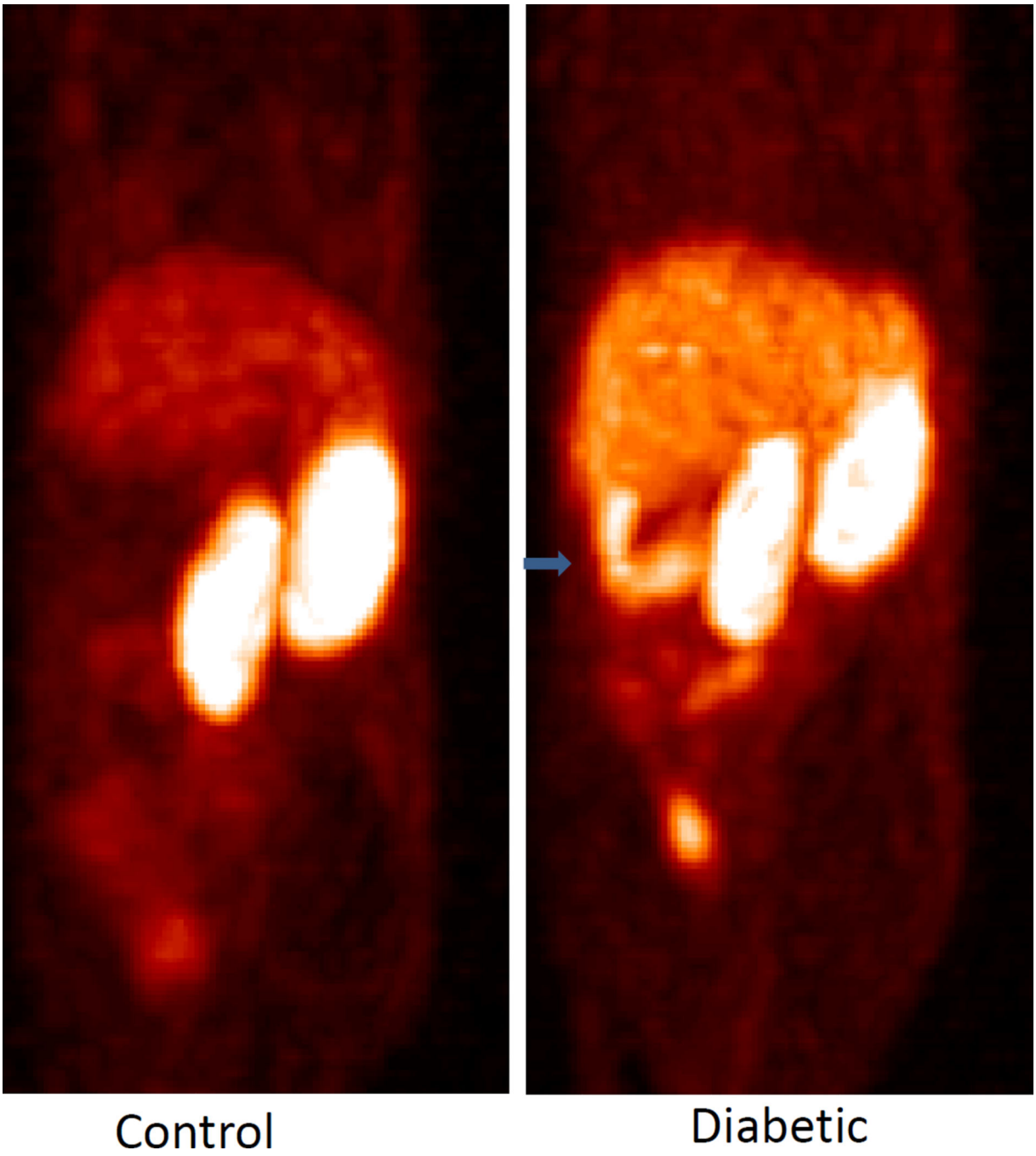

Figure 3.

In vivo PET images obtained 24 h after administration of ^{64}Cu-labelled cFLFLF to a control (left panel) and a diabetic mouse (right panel). The peptide was administered via the tail veins. The arrow sign (→) denotes the pancreas. Diabetic mice showed an increased tracer accumulation in the pancreas and the liver compared to the control mice.

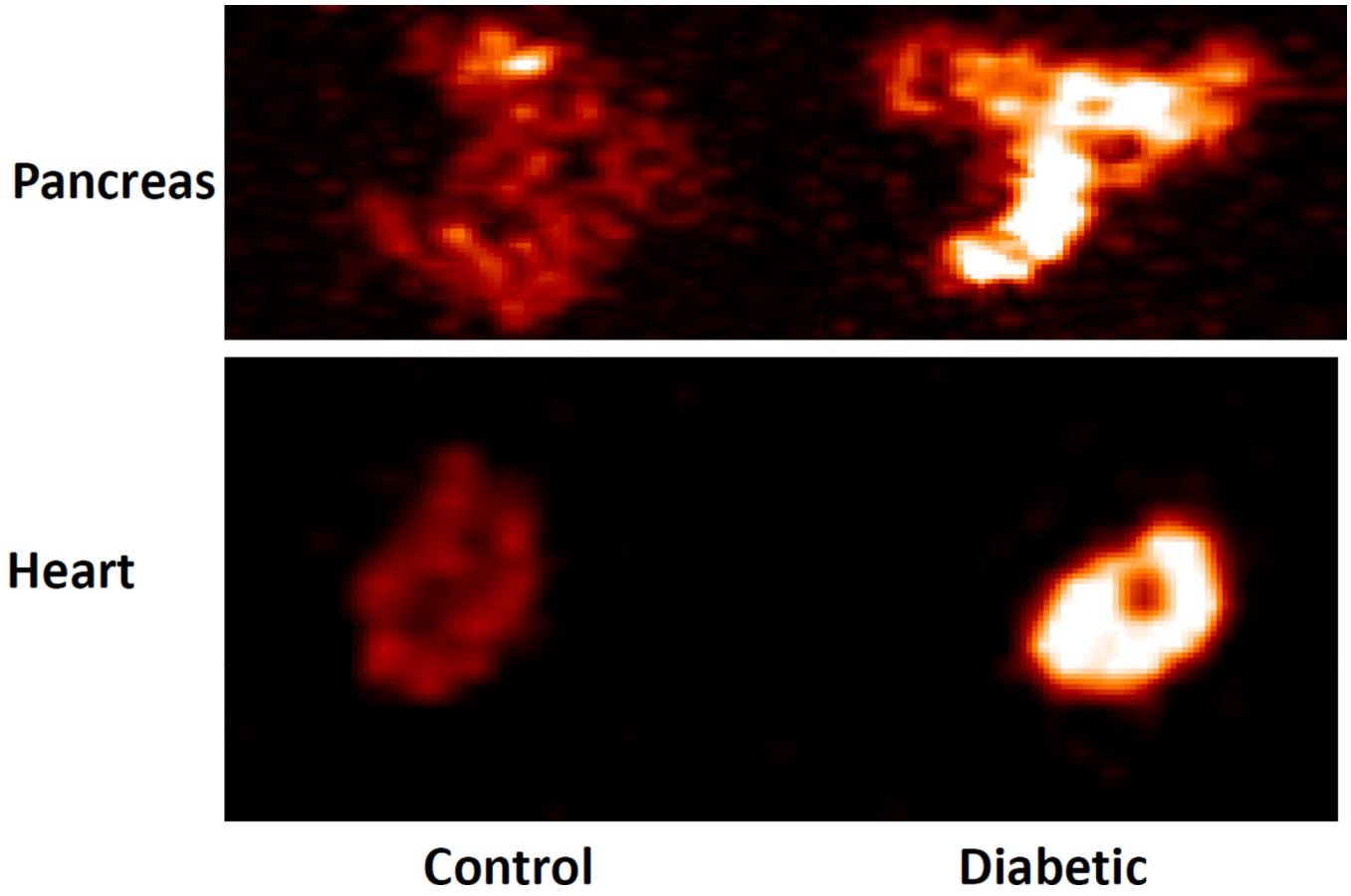

Figure 4.

Representative ex vivo PET images of the isolated heart and pancreas from a control and a diabetic mouse. Immediately following in vivo PET scans, the heart and pancreas were removed from the mice and PET scans performed on the isolated organs. The diabetic heart and pancreas showed more tracer retention than the control heart and pancreas, respectively.

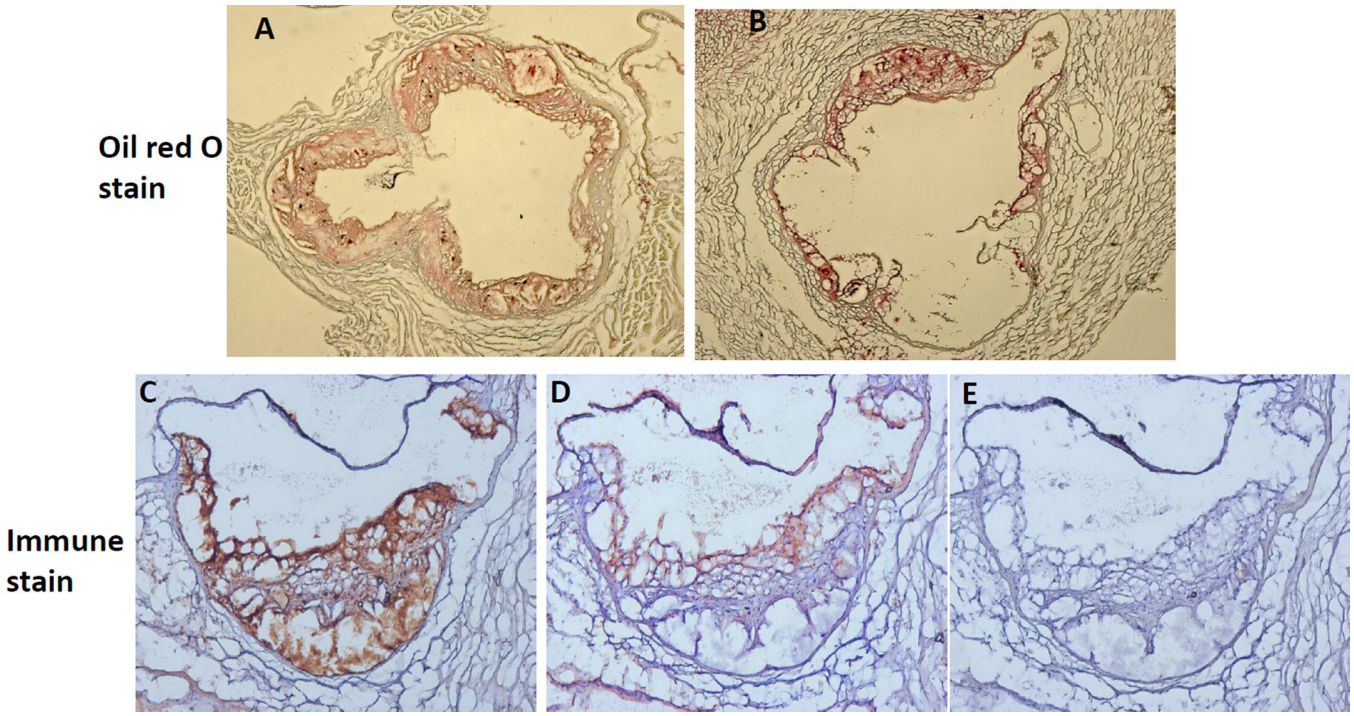

Figure 5.

Top panels: Oil red O staining of atherosclerotic lesions in the aortic root of the heart that underwent ex vivo PET scans. The aortic root was cross-sectioned and the sections were stained with oil red O. Diabetic mice (A) had much larger atherosclerotic lesions than control mice (B). Lower panels: cross-sections of the aortic root of a diabetic mouse stained with a specific antibody against macrophages (C) or FPR1 (D). E, negative control for immune stain. A and B, original magnification X4; C thru E, magnification X10.

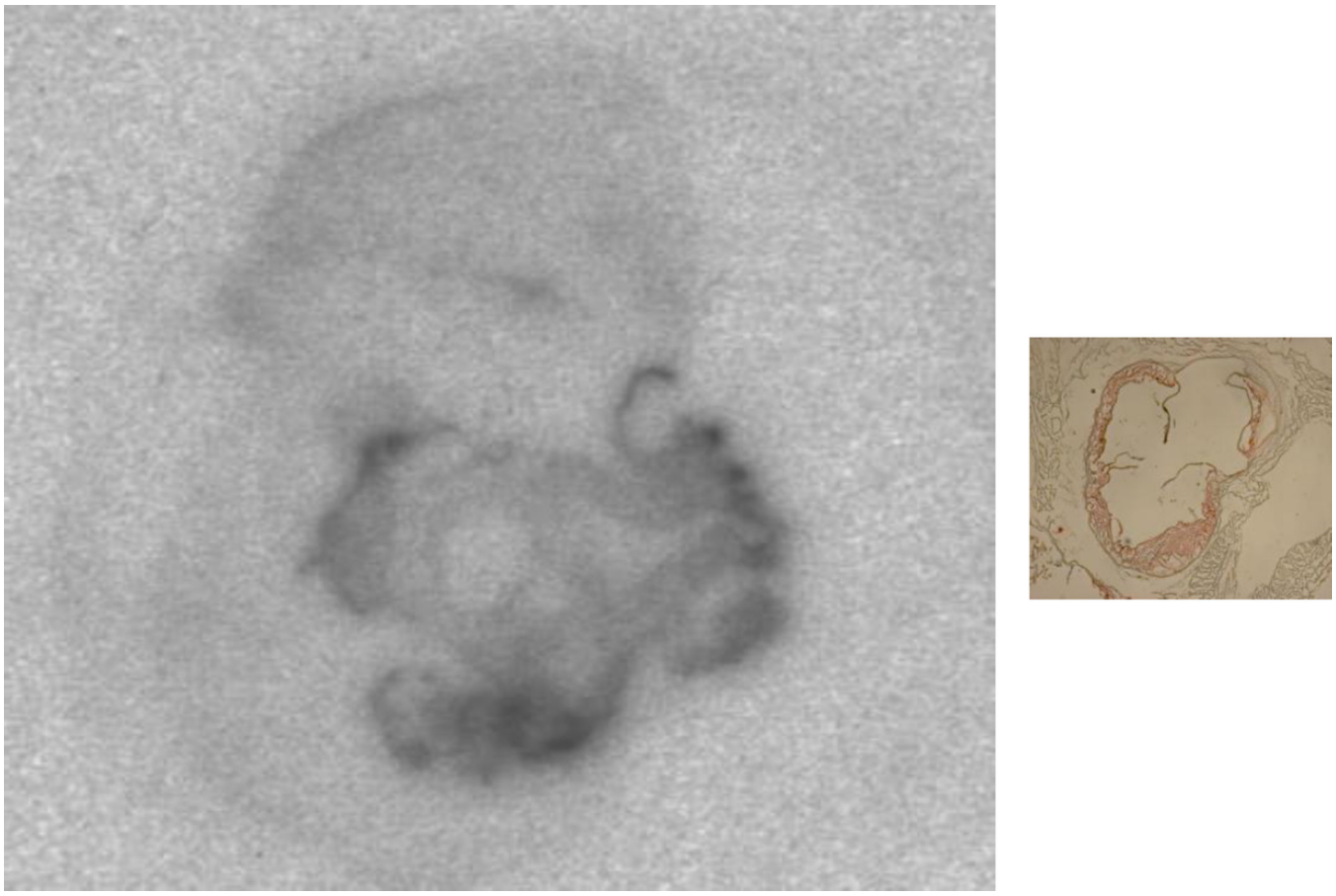

Figure 6.

An autoradiographic image of an aortic root section incubated with ^{64}Cu-cFLFLFK and an adjacent section stained with oil red O showing plaue presence. The aortic root was from Apoe$^{-/-}$ mouse fed the Western diet. The area with atherosclerotic lesions shows strong radioactivity.

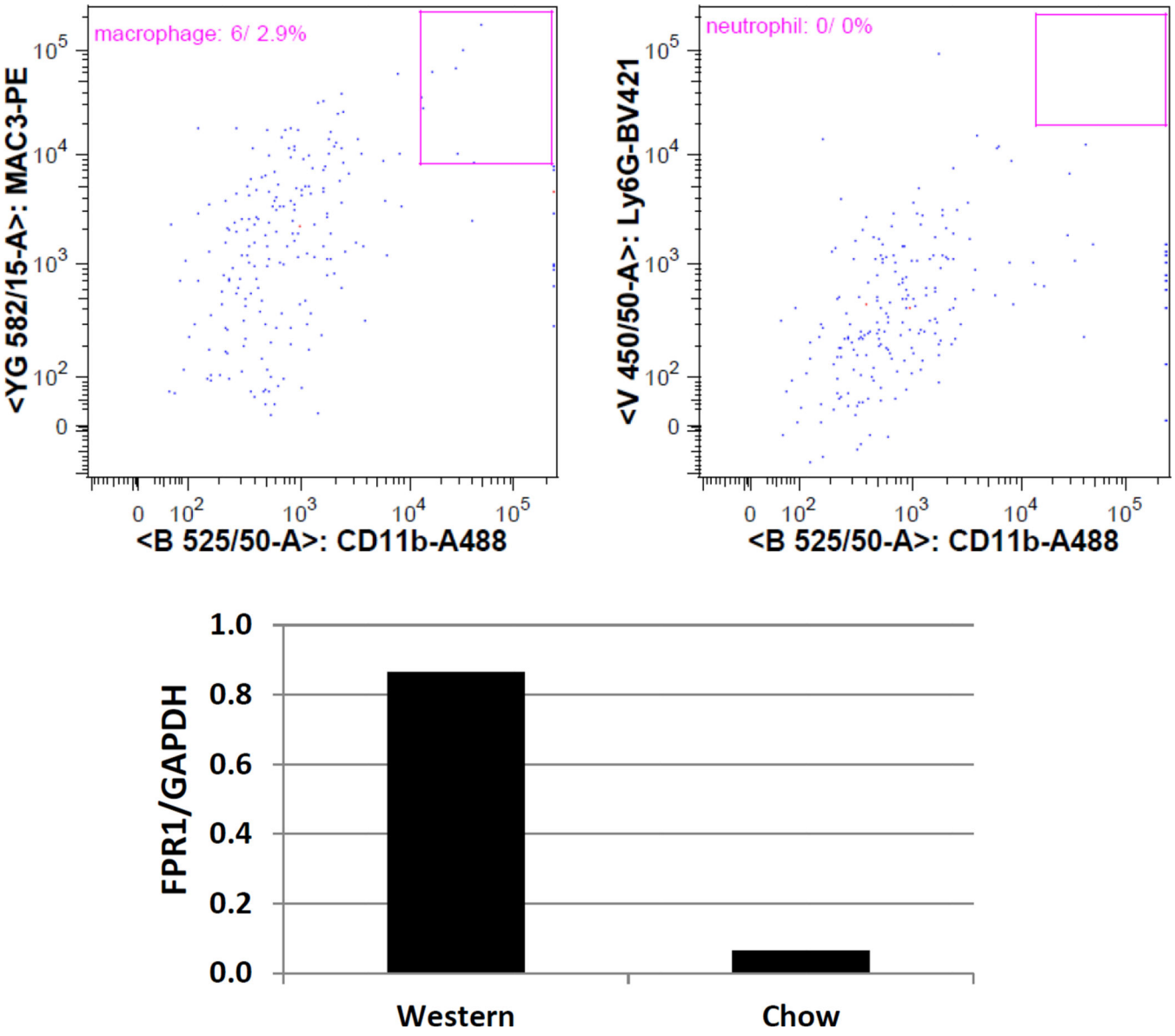

Figure 7.

Upper panels: Flow cytometric analysis of macrophages and neutrophils in the islets of B6.Apoe$^{-/-}$mice fed the Western diet. Macrophages were identified as CD11b and Mac3 double positive cells gated for CD45. Neutrophils were identified as CD11b and LY-6G positive cells gated for CD45. Lower panel: Real-time PCR analysis of FPR1 expression in pancreatic islets of mice fed a chow or Western diet. Gene expression levels are expressed as a ratio of FPR1 mRNA relative to GAPDH mRNA.